Effect of geometric lattice design on optical/electrical properties of transparent silver grid for organic solar cells

Ju Won Lim,[1,2] Young Tack Lee,[1] Rina Pandey,[1,3] Tae-Hee Yoo,[1,4] Byoung-In Sang,[4] Byeong-Kwon Ju,[2,5] Do Kyung Hwang,[1,3,*] and Won Kook Choi[1,3,6]

[1] *Interface Control Research Center, Future Convergence Research Division, Korea Institute of Science and Technology (KIST), Seongbuk Gu, Hwarangro 14 Gil 5, Seoul, 136-791, South Korea*
[2] *Displays and Nanosystem Laboratory, College of Engineering, Korea University, Seoul 136-713, South Korea*
[3] *Department of Nanomaterials Science and Engineering, Korean University of Science and Technology (KUST), Yuseong Gu, Gajeong-ro 217, Daejeon 305-350, South Korea*
[4] *Department of Chemical Engineering, Hanyang University, Seoul 133-791, South Korea*
[5] *bkju@korea.ac.kr*
[6] *wkchoi@kist.re.kr*
[*] *dkhwang@kist.re.kr*

Abstract: Silver (Ag) grid transparent electrode is one of the most promising transparent conducting electrodes (TCEs) to replace conventional indium tin oxide (ITO). We systematically investigate an effect of geometric lattice modifications on optical and electrical properties of Ag grid electrode. The reference Ag grid with 5 μm width and 100 μm pitch (duty of 0.05) prepared by conventional photo-lithography and lift-off processes shows the sheet resistance of 13.27 Ω/sq, transmittance of 81.1%, and resultant figure of merit (FOM) of 129.05. Three different modified Ag grid electrodes with stripe added-mesh (SAM), triangle-added mesh (TAM), and diagonal-added mesh (DAM) are suggested to improve optical and electrical properties. Although all three of SAM, TAM, and DAM Ag grid electrodes exhibit the lower transmittance values of about 72 - 77%, they showed much decreased sheet resistance of 6 - 8 Ω/sq. As a result, all of the lattice-modified Ag grid electrodes display significant improvement of FOM and the highest value of 171.14 is obtained from DAM Ag grid, which is comparable to that of conventional ITO electrode (175.46). Also, the feasibility of DAM Ag gird electrode for use in organic solar cell is confirmed by finite difference time domain (FDTD) simulations. Unlike a conventional ITO electrode, DAM Ag grid electrode can induce light scattering and trapping due to the diffuse transmission that compensates for the loss in optical transparency, resulting in comparable light absorption in the photo active layer of poly(3-hexylthiophene) (P3HT): [6,6]-phenyl-C61-butyric acid methyl ester ($PC_{60}BM$). P3HT:$PC_{60}BM$ based OSCs with the DAM Ag grid electrode were fabricated, which also showed the potential for ITO-free transparent electrode.

OCIS codes: (350.6050) Solar energy; (040.5350) Photovoltaic; (310.6860) Thin films, optical properties; (310.7005) Transparent conductive coatings.

References and links

1. T. Hamaguchi, K. Omae, T. Takebayashi, Y. Kikuchi, N. Yoshioka, Y. Nishiwaki, A. Tanaka, M. Hirata, O. Taguchi, and T. Chonan, "Exposure to hardly soluble indium compounds in ITO production and recycling plants is a new risk for interstitial lung damage," Occup. Environ. Med. **65**(1), 51–55 (2008).
2. B. Kippelen and J.-L. Bredas, "Organic photovoltaics," Energy Environ. Sci. **2**(3), 251–261 (2009).
3. K.-D. Chang, C.-Y. Li, J.-W. Pan, and K.-Y. Cheng, "A hybrid simulated method for analyzing the optical efficiency of a head-mounted display with a quasi-crystal OLED panel," Opt. Express **22**(S2), A567–A576

#224594 - $15.00 USD Received 9 Oct 2014; accepted 13 Oct 2014; published 22 Oct 2014

(2014).
4. K.-H. Lee, S.-M. Kim, H. Jeong, Y. Pak, H. Song, J. Park, K.-H. Lim, J.-H. Kim, Y. S. Kim, H. C. Ko, I. K. Kwon, and G.-Y. Jung, "All-solution-processed transparent thin film transistor and its application to liquid crystals driving," Adv. Mater. **25**(23), 3209–3214 (2013).
5. P. Kuang, J.-M. Park, W. Leung, R. C. Mahadevapuram, K. S. Nalwa, T.-G. Kim, S. Chaudhary, K.-M. Ho, and K. Constant, "A new architecture for transparent electrodes: relieving the trade-off between electrical conductivity and optical transmittance," Adv. Mater. **23**(21), 2469–2473 (2011).
6. T. Minami, "Substitution of transparent conducting oxide thin films for indium tin oxide transparent electrode applications," Thin Solid Films **516**(7), 1314–1321 (2008).
7. Z. Chen, B. Cotterell, W. Wang, E. Guenther, and S. J. Chua, "A mechanical assessment of flexible optoelectronic devices," Thin Solid Films **394**(1–2), 201–205 (2001).
8. V. E. Ferry, A. Polman, and H. A. Atwater, "Modeling light trapping in nanostructured solar cells," ACS Nano **5**(12), 10055–10064 (2011).
9. B. Park and H. G. Jeon, "Spontaneous buckling in flexible organic light-emitting devices for enhanced light extraction," Opt. Express **19**(S5), A1117–A1125 (2011).
10. M. Vosgueritchian, D. J. Lipomi, and Z. Bao, "Highly conductive and transparent pedot:pss films with a fluorosurfactant for stretchable and flexible transparent electrodes," Adv. Funct. Mater. **22**(2), 421–428 (2012).
11. R. V. Salvatierra, C. E. Cava, L. S. Roman, and A. J. G. Zarbin, "ITO-free and flexible organic photovoltaic device based on high transparent and conductive polyaniline/carbon nanotube thin films," Adv. Funct. Mater. **23**(12), 1490–1499 (2013).
12. B.-J. Kim, M. A. Mastro, J. Hite, C. R. Eddy, Jr., and J. Kim, "Transparent conductive graphene electrode in GaN-based ultra-violet light emitting diodes," Opt. Express **18**(22), 23030–23034 (2010).
13. S. Bae, H. Kim, Y. Lee, X. Xu, J.-S. Park, Y. Zheng, J. Balakrishnan, T. Lei, H. R. Kim, Y. I. Song, Y.-J. Kim, K. S. Kim, B. Ozyilmaz, J.-H. Ahn, B. H. Hong, and S. Iijima, "Roll-to-roll production of 30-inch graphene films for transparent electrodes," Nat. Nanotechnol. **5**(8), 574–578 (2010).
14. H. Eom, J. Lee, A. Pichitpajongkit, M. Amjadi, J.-H. Jeong, E. Lee, J.-Y. Lee, and I. Park, "Ag@Ni core–shell nanowire network for robust transparent electrodes against oxidation and sulfurization," Small **10**(20), 4171–4181 (2014).
15. S. Lee, D. R. Mason, S. In, and N. Park, "Embedding metal electrodes in thick active layers for ITO-free plasmonic organic solar cells with improved performance," Opt. Express **22**(S4), A1145–A1152 (2014).
16. J. van de Groep, P. Spinelli, and A. Polman, "Transparent conducting silver nanowire networks," Nano Lett. **12**(6), 3138–3144 (2012).
17. C. F. Guo, T. Sun, Q. Liu, Z. Suo, and Z. Ren, "Highly stretchable and transparent nanomesh electrodes made by grain boundary lithography," Nat. Commun. **5**, 3121 (2014).
18. S. De, T. M. Higgins, P. E. Lyons, E. M. Doherty, P. N. Nirmalraj, W. J. Blau, J. J. Boland, and J. N. Coleman, "Silver nanowire networks as flexible, transparent, conducting films: extremely high dc to optical conductivity ratios," ACS Nano **3**(7), 1767–1774 (2009).
19. M.-G. Kang, M.-S. Kim, J. Kim, and L. J. Guo, "Organic solar cells using nanoimprinted transparent metal electrodes," Adv. Mater. **20**(23), 4408–4413 (2008).
20. A. I. Mares and J. M. van Ruitenbeek, "Observation of shell effects in nanowires for the noble metals Cu, Ag, and Au," Phys. Rev. B **72**(20), 205402 (2005).
21. J. Zou, H.-L. Yip, S. K. Hau, and A. K. Y. Jen, "Metal grid/conducting polymer hybrid transparent electrode for inverted polymer solar cells," Appl. Phys. Lett. **96**(20), 203301 (2010).
22. H.-J. Kim, S.-H. Lee, J. Lee, E.-S. Lee, J.-H. Choi, J.-H. Jung, J.-Y. Jung, and D.-G. Choi, "High-durable agni nanomesh film for a transparent conducting electrode," Small **10**(18), 3767–3774 (2014).
23. S. Hong, J. Yeo, G. Kim, D. Kim, H. Lee, J. Kwon, H. Lee, P. Lee, and S. H. Ko, "Nonvacuum, maskless fabrication of a flexible metal grid transparent conductor by low-temperature selective laser sintering of nanoparticle ink," ACS Nano **7**(6), 5024–5031 (2013).
24. N. Kwon, K. Kim, S. Sung, I. Yi, and I. Chung, "Highly conductive and transparent ag honeycomb mesh fabricated using a monolayer of polystyrene spheres," Nanotechnology **24**(23), 235205 (2013).
25. Y. Galagan, J.-E. J. M. Rubingh, R. Andriessen, C.-C. Fan, P. W. M. Blom, S. C. Veenstra, and J. M. Kroon, "ITO-free flexible organic solar cells with printed current collecting grids," Sol. Energy Mater. Sol. Cells **95**(5), 1339–1343 (2011).
26. M. Layani, A. Kamyshny, and S. Magdassi, "Transparent conductors composed of nanomaterials," Nanoscale **6**(11), 5581–5591 (2014).
27. Y. Zhou, L. B. Hu, and G. Gruner, "A method of printing carbon nanotube thin films," Appl. Phys. Lett. **88**(12), 123109 (2006).
28. I. Kim, T. S. Lee, D. S. Jeong, W. S. Lee, W. M. Kim, and K.-S. Lee, "Optical design of transparent metal grids for plasmonic absorption enhancement in ultrathin organic solar cells," Opt. Express **21**(S4), A669–A676 (2013).
29. H. A. Atwater and A. Polman, "Plasmonics for improved photovoltaic devices," Nat. Mater. **9**(3), 205–213 (2010).

#224594 - $15.00 USD Received 9 Oct 2014; accepted 13 Oct 2014; published 22 Oct 2014

1. Introduction

Transparent conducting electrodes (TCEs) play a vital role in today's many optoelectronic applications of liquid crystal display (LCD), organic lighting emitting diode (OLED) display, touch screen, and solar cells [1–4]. Until now, indium tin oxide (ITO) is widely used as the transparent electrode material because it satisfies electrical and optical requirements for fabrication of various optoelectronic devices. Recently, however, ITO suffers from several drawbacks [5–8]: (1) increased price due to rising demand and diminishing production of indium, (2) brittle nature which makes it not suitable for flexible and wearable applications, and (3) strong absorption region in UV/blue spectral range which is problematic in a further improvement of efficiency in solar cells.

In order to solve these problems, much effort has been devoted to develop new TCE materials to replace ITO. Many different types of materials such as conducting polymers [9,10], carbon nanotubes [11], graphene [12,13], metal nanowire [14], and metal grids [15–17] have been proposed. Among the alternative transparent electrodes, metal grid electrode is a promising candidate because of its very high electrical conductivity, good optical transparency, and mechanical stability [18–21]. Two main issues of metal grid electrode are the selection of materials and the optimization of mesh dimension such as width and pitch. For metal selection, silver (Ag) grid is regarded as one of the best options, considering low-cost, process ability, excellent optical and electrical properties despite its relatively low chemical stability and long-term stability [20–23]. Recent research works of Ag grid electrode have focused on the optimization of dimension by reducing width and pitch under sub-micrometer scale to achieve high optical transparency and electrical conductivity [16,21]. However, such downscaling brings about increased process cost and technical limitation.

In the study, we systematically investigated an effect of geometric lattice modifications on optical and electrical properties of Ag grid electrode and suggested an optimized design within micrometer scale for TCE. The reference silver grid with 5 μm width and 100 μm pitch (duty of 0.05) showed the sheet resistance of 13.27 Ω/sq, transmittance of 81.1%, and resultant figure of merit (FOM) of 129.05. Stripe-added mesh (SAM), triangle-added mesh (TAM), and diagonal-added mesh (DAM) Ag grid electrodes with simple lattice modification were fabricated to improve the optical and electrical properties. Although the optical transparency of all SAM, TAM, and DAM Ag grid electrodes reduced (72 - 77%), much decreased sheet resistance values of 6 - 8 Ω/sq were obtained by shortening electron paths with optimized charge collection [24,25]. Such enhancement of electrical conductivity of SAM, TAM, and DAM Ag grid electrodes over-compensated for the reduction in optical transparency, resulting in the improvement in FOM. The highest FOM value of 171.14 is obtained from DAM Ag grid, which is comparable to that of conventional ITO electrode (175.46). In order to examine the feasibility of DAM Ag grid electrode for use in organic solar cell, finite difference time domain (FDTD) simulations were carried out. Unlike a conventional ITO electrode, the use of DAM Ag grid electrode can facilitate light scattering and trapping due to the diffuse transmission that compensates for the loss in optical transparency, resulting in comparable light absorption in the photo active layer of poly(3-hexylthiophene) (P3HT): [6,6]-phenyl-C61-butyric acid methyl ester ($PC_{60}BM$). We fabricated P3HT:$PC_{60}BM$ based OSCs with the DAM Ag grid electrode that also showed the potential for ITO-free transparent electrode.

2. Experimental methods

Schematic illustration of Ag grid film process is shown in Fig. 1. A lift off resist (LOR 3A) was deposited on a glass substrate (Corning Eagle) by spin coating at 4000 rpm for 40 sec and prebaked at 165°C for 3 min. Then, positive photoresist (PR) (AZ GXR-601) was deposited by spin coating at 3000 rpm for 30 sec and prebaked at 115°C for 1 min. Four different grid dimensions and shapes were patterned by conventional photolithography. The 50 nm-thick

#224594 - $15.00 USD Received 9 Oct 2014; accepted 13 Oct 2014; published 22 Oct 2014

Ag thin films were deposited by radio frequency (rf) magnetron sputtering system. Finally, four different Ag grid films were patterned through lift-off process.

Organic solar cells (OSCs) were fabricated on ITO/glass and Ag grid mesh/glass substrates. 100 nm-thick PEDOT:PSS (CleviosTM P VP AI 4083) layers were deposited on the top of the ITO and Ag grid mesh by spin coating at 4000 rpm for 40 s using the solution mixed with methanol (Aldrich) at a weight ratio of 1:1. Then the sample was annealed on a hot plate at 130 °C for 30 min in a glove box. 18 mg of P3HT (Rieke metals, Inc.) and 10.8 mg of PC60BM were dissolved in 1 ml of chlorobenzene solvent. The P3HT:PC_{60}BM layer was spin coated at 2500 rpm for 40 s and was annealed at 150 °C for 10 min in the glove box. Finally, the electron collecting and top electrode (LiF/Al) were deposited by a thermal evaporation system.

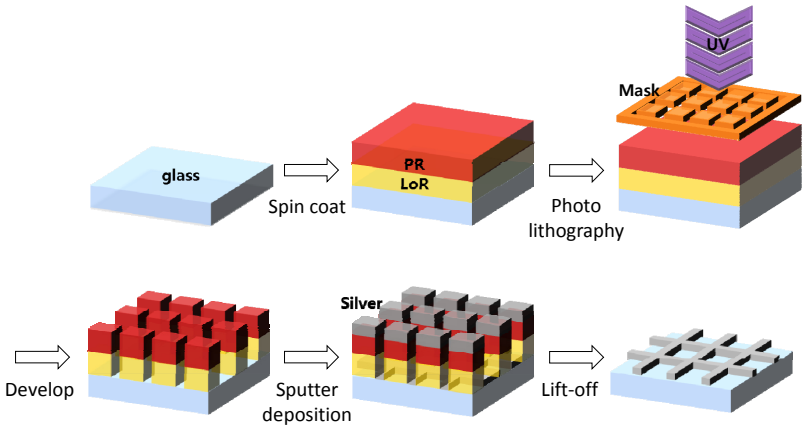

Fig. 1. Schematic illustration of Ag grid film process.

3. Results and discussions

Figures 2(a)–2(d) show optical microscope images of the four different Ag grid films on glass substrates. In the reference Ag grid film, line width of Ag and pitch were 5 μm and 100 μm, respectively [see Fig. 2(a)]. In general, duty is defined as the ratio of line width to pitch and its value of the reference Ag grid film is 0.05. The three different modified Ag grid electrodes with SAM, TAM, and DAM were prepared to investigate variation of optical and electrical properties. SAM geometry is simple addition of a strip line on the reference grid structure as shown in Fig. 2(b), resulting in the reduction of pitch (50 μm) and duty (0.1). TAM structure consists of equilateral triangles on spacing of 100 μm vertical line [see Fig. 2(c)]. Diagonal line is added on the reference grid and it can be DAM grid structure that is composed of right triangles on spacing of 100 μm vertical line similar to TAM grid, as shown in Fig. 2(d). All the structures of the Ag grid electrodes have same line width of 5 μm and film thickness of 50 nm.

#224594 - $15.00 USD Received 9 Oct 2014; accepted 13 Oct 2014; published 22 Oct 2014

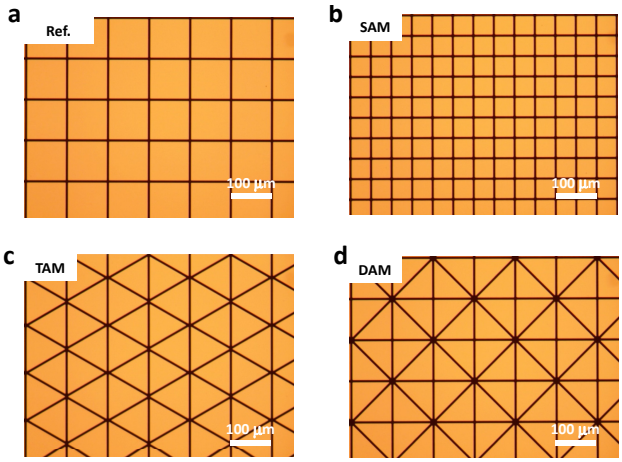

Fig. 2. Optical microscope images of (a) reference, (b) SAM, (c) TAM, (d) DAM Ag grid films on glass substrates.

Figure 3(a) shows optical transmittance spectra of the all Ag grid films in the range of 380 - 800 nm, which were measured with an ultraviolet-visible spectrometer (Perkin Elmer UV/Vis spectrometer Lambda 18). Reference Ag grid film has the averaged transmittance of 81.1%. In comparison with the reference, all of SAM, TAM, and DAM Ag grid films have the lower transmittance of 72.7%, 76.6%, and 74.9%, which are attributed to the reduced open area without metal lines in a unit cell. However, although SAM, TAM, DAM Ag grid films had lost some optical transparency, the electrical conductivities of these modified grid films have significantly improved, as shown in Fig. 3(b), which shows average transmittances as a function of sheet resistances. The sheet resistances were measured by a 4-point probe method with a Keithley 2400 source meter. Unlike the optical transparency, the electrical conductivity is inversely proportional to aforementioned open area that is likely to act as non-conductive void [26]. The SAM grid film has twice smaller pitch values than that of the reference grid film which means that electron conducting paths are shorter. As a result, the SAM grid film exhibited significantly reduced sheet resistance value of 6.61 Ω/sq (enhanced electrical conductivity) while the reference sample showed sheet resistance value of 13.27 Ω/sq Similarly, TAM and DAM grid films also displayed the decreased sheet resistance of which value were 7.75 and 7.07 Ω/sq, respectively.

Based on the above results, there is a trade-off relationship between optical transparency and electrical conductivity in the Ag grid films. In order to evaluate the overall performance as a transparent conductor and find optimized grid design considering both optical and electrical properties, figures of merit (FOM) defined as the ratio between the electrical conductance and the optical conductance (σ_{DC}/σ_{opt}) were calculated. The FOM is given by following equation [16,27],

$$T = \left(1 + \frac{188.5}{R_s}\frac{\sigma_{opt}}{\sigma_{dc}}\right)^{-2}. \quad (1)$$

where R_s is the sheet resistance and T is the averaged transmittance, respectively. The values of FOM for all four different Ag grid films are shown in Fig. 3(c) (note: the FOM of ITO is calculated from transmittance and sheet resistance of 85.7% and 13.36 Ω/sq, respectively, and its value marked with the horizontal sky-blue dashed line for comparison). The FOM value obtained from the reference grid film is 129.05, much lower than that of ITO (175.46). However, all three modified Ag grid film showed significant improvement in FOM. This means that the enhancement of electrical conductivity over-compensates for the reduction in

#224594 - $15.00 USD Received 9 Oct 2014; accepted 13 Oct 2014; published 22 Oct 2014

optical transparency, resulting in the overall improvement in FOM. Among the three modified Ag grid film, the DAM grid geometry is likely to be the most optimized lattice modification, which has the highest FOM value of 171.41 comparable to that of conventional ITO electrode. Figure 3(d) exhibits photographs of ITO (left side) and DAM Ag grid (right side) films on glass substrates placed on our institute emblem that can clearly be identified by naked eyes. Details on the optical and electrical parameters of transmittance, sheet resistance, and figure of merit obtained from all of reference, SAM, TAM, DAM Ag grid and ITO films are summarized in Table 1.

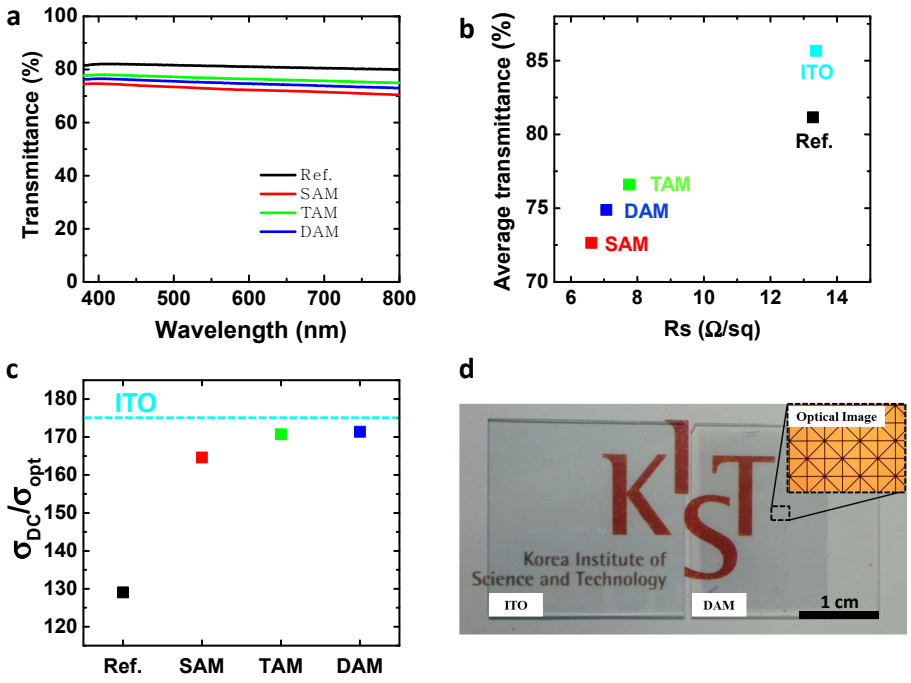

Fig. 3. (a) Optical transmittance spectra of reference, SAM, TAM and DAM Ag grid films in the range of 380 - 800 nm. (b) Average transmittance as a function of sheet resistance and (c) figure of merit defined as the ratio of the electrical conductance and the optical conductance (σ_{DC} / σ_{opt}) as a function of grid geometry. (d) Photographs of ITO and DAM Ag grid film placed on our institute emblem.

Table 1. Optical and electrical parameters of transmittance, sheet resistance, and figure of merit obtained from reference, SAM, TAM, DAM Ag grid and ITO films

	Ref.	SAM	TAM	DAM	ITO
Transmittance (%) (380-800 nm)	81.1	72.7	76.6	74.9	85.7
Sheet resistance (Ω/□)	13.27	6.61	7.75	7.07	13.36
Figure of merit	129.05	164.61	170.18	171.41	175.46

#224594 - $15.00 USD Received 9 Oct 2014; accepted 13 Oct 2014; published 22 Oct 2014

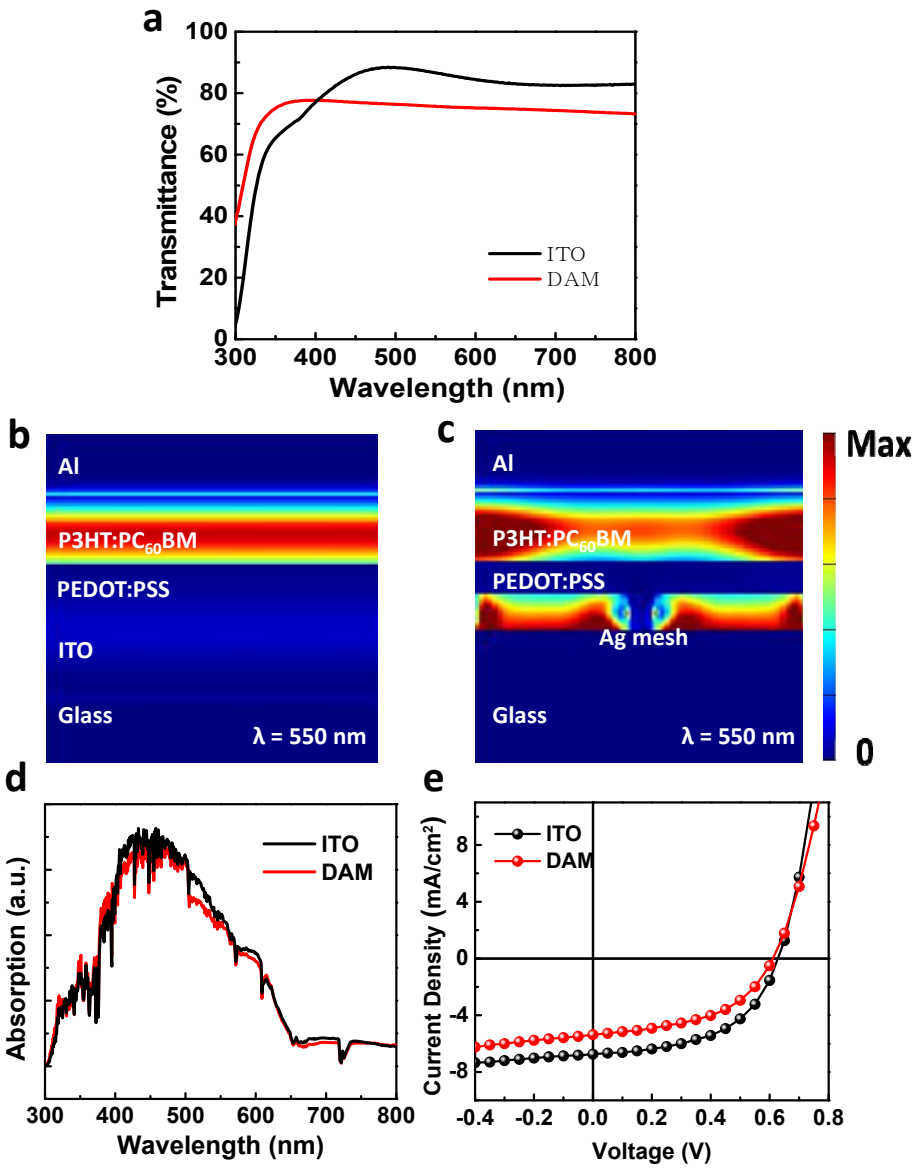

Fig. 4. FDTD simulation and real device results. (a) Simulated transmittance spectra of ITO and DAM Ag grid films. Light absorption maps in the OSCs with (b) ITO and (c) DAM Ag grid electrodes. (d) Calculated the total absorption spectra of photoactive layers in the devices with ITO and DAM Ag grid electrodes. (e) Representative J-V characteristics of an PTB7:PC70BM OSC with the Ag grid electrode and the ITO electrode device under AM 1.5 G illumination with 100 mW/cm^2 intensity.

The Ag grid TCE can be employed for organic solar cells (OSCs) as a possible application. The DAM Ag grid electrode was chosen and the feasibility was examined by FDTD simulation. Firstly, the transmittance spectra of ITO and DAM Ag grid films were calculated, as shown in Fig. 4(a). The average transmittance values were estimated to be 85.6% for ITO and 74.8 for DAM Ag grid, which are consistent with experimentally measured values. For the next step, the light absorption in each layer of OSCs under a 550 nm wavelength plane light source is calculated. Figures 4(b) and 4(c) depict the simulated light

#224594 - $15.00 USD Received 9 Oct 2014; accepted 13 Oct 2014; published 22 Oct 2014

absorption maps in OSCs with ITO or a Ag grid, poly(3,4-ethylenedioxythiophene): poly(styrenesulfonate) (PEDOT:PSS) as the hole collecting layer, P3HT:PC_{60}BM as the photo active layer, and Al as the top electrode. In general, the light absorption in photo active layer that significantly affects the OSC performance is proportional to the optical transparency of the TCE. However, based on the simulated maps, the total amounts of light absorption in photo active layer with OSCs using ITO and DAM Ag grid electrode are likely to be comparable although non-uniform light absorption in the photo active layer is observed in the device with the DAM Ag grid. Such enhancement in OSCs with Ag grid electrode is inconsistent with the transmittance results above but can be explained by scattering and trapping effect due to the Ag grid geometry [28,29]. Unlike a conventional ITO, the incident light is substantially scattered by the Ag grid due to the diffuse transmission, which is confirmed by the distorted light absorption in the Ag grid layer. Then, the scattered light is reflected by the top Al metal electrode and re-scattered/re-reflected by the DAM Ag grid. Through repetitions of this process, the light is trapped in the device that can compensate for the lower optical transmittance of the DAM Ag grid film. Based on the above results of the absorption maps, the total absorption spectra in the range of 300 - 800 nm can be calculated as shown in Fig. 4(d). The figure shows that the light absorption of both the ITO and Ag grid of photo active layers would be almost identical, due to the light scattering and trapping induced by Ag grid. We also fabricated P3HT:PC_{60}BM OSCs with ITO and DAM grid electrodes. Figure 4(e) exhibits the current density-voltage (*J-V*) characteristics of the OSC with the DAM Ag grid electrode and the reference device with ITO electrode under AM 1.5 G illumination. The device with the DAM Ag grid electrode shows almost similar open circuit voltage (V_{oc}), fill factor (FF) compared with the reference ITO electrode device. However, the short circuit current density (J_{sc}) of the DAM electrode device is slightly lower than that of ITO device, resulting in less power conversion efficiency (PCE): 1.62% for the DAM and 2.22% for the ITO. In the real OSCs, the device performance is involved in many factors such as light absorption, charge collection, exciton diffusion, and so on, but our FDTD simulation considered only light absorption. The lower J_{sc} with the DAM Ag grid electrode is likely to result from relatively low charge collection efficiency due to non-conductive voids in the mesh film. Filling these non-conductive voids of the Ag grid with conducting materials such as highly conducting PEDOT:PSS (e.g. PH1000 by Heraeus) can enhance charge collection efficiency, resulting in the improvement of device performance. In addition, when one considers other influential factors, the performance of the device with the DAM grid electrode may be further enhanced if the process condition is more optimized.

4. Conclusion

In summary, we systematically investigated an effect of geometric lattice modifications on optical and electrical properties of Ag grid electrode and found the optimized grid structure. The reference silver grid with 5 μm width and 100 μm pitch (duty of 0.05) showed sheet resistance of 13.27 Ω/sq, transmittance of 81.1%, and resultant figure of merit (FOM) of 129.05. SAM, TAM, and DAM Ag grid electrodes with simple lattice modification were suggested to improve the optical and electrical properties. Although the optical transparencies of all SAM, TAM, and DAM Ag grid electrodes have been reduced (72 - 77%), much decreased sheet resistance values of 6 - 8 Ω/sq were obtained by shortening electron paths with optimized charge collection. Such enhancement of electrical conductivity of SAM, TAM, and DAM Ag grid electrodes over-compensated for the reduction in optical transparency, resulting in the improvement in FOM. Among the three modified Ag grid film, the DAM grid geometry was one of the effective geometric lattice designs, which has the highest FOM value of 171.41, comparable to that of a conventional ITO electrode (175.46). Finally, the feasibility of DAM Ag grid electrode for use in organic solar cell was confirmed by FDTD simulations. Unlike a conventional ITO electrode, the use of DAM Ag grid electrode can facilitate light scattering and trapping due to the diffuse transmission that

#224594 - $15.00 USD Received 9 Oct 2014; accepted 13 Oct 2014; published 22 Oct 2014

compensates for the loss in optical transparency, resulting in comparable absorption spectra of photoactive layers (P3HT:$PC_{60}BM$) in the devices with ITO and DAM Ag grid electrodes. In addition, P3HT:$PC_{60}BM$ based OSCs with the DAM Ag grid electrode were fabricated, which also showed the potential for ITO-free transparent electrode. Based on our results, optical and electrical properties of Ag grid films can be tuned by simple lattice modification to satisfy requirements for optoelectronic device applications. We thus conclude that Ag grid electrode is a promising transparent electrode to replace ITO electrode, allowing for further development of low cost, highly efficient, and large-scale OSC modules.

Acknowledgments

The author D. K. Hwang and W. K. Choi, would like to appreciate for the financial support by the Converging Research Center Program through the Ministry of Science and ICT and Future Planning, Korea (Grant No. NRF-2009-0082023), KIST Institution Program (Grant No. 2E24871), and Industrial Core Technology Development Program from Ministry of Trade, Industry & Energy (Grant No. 10035616 and 10035648).